

NJC

New Journal of Chemistry

An international journal of the chemical sciences

Redox-Driven Switching in Pseudorotaxanes

Ali Trabolsi,^a Mohamad Hmadeh,^b Niveen M. Khashab,^a Douglas C. Friedman,^a Matthew E. Belowich,^a Nicolas Humbert,^b Mourad Elhabiri,^b Hussam A. Khatib,^a Anne-Marie Albrecht-Gary*^b and J. Fraser Stoddart*^a

^a Department of Chemistry, Northwestern University, 2145 Sheridan Road, Evanston, Il, 60208, USA. Fax :

(+1)-847-491-1009, Tel : (+1)-847-491-3793

E-mail: stoddart@northwestern.edu

^b Laboratoire de Physico-Chimie Bioinorganique, ULP-CNRS (UMR 7177), Institut de Chimie, ECPM, 25 rue Becquerel, 67200 Strasbourg, France.

Fax: (+33)-3-90-24-26-39, Tel: (+33)-3-90-24-26-38

E-mail: amalbre@chimie.u-strasbg.fr

Revised Version

Supplementary Information

* To whom correspondence should be addressed

Introduction

In this Supplement, we describe the spectroscopic characterization of the inclusion complexes of the two threads **1**·4Cl and **2**·2Cl with cucurbit[8]uril (designated **CB[8]**). This extensive physico-chemical study requires, first of all, the examination of model compounds – namely, a monotopic dicationic system **V**·2Cl acting as a π -electron accepting unit and two π -electron donating counterparts **N-1** or **N-2**. Their host-guest complexes ($\text{V}^{2+} \subset \text{CB[8]}$, $\text{V}^{2+} \cdot \text{N-1} \subset \text{CB[8]}$ and $\text{V}^{2+} \cdot \text{N-2} \subset \text{CB[8]}$) with **CB[8]** were characterized using spectroscopic techniques (absorption and emission) which are described herein.

Figure S1 shows the absence of dilution effects on the charge transfer (CT) absorption bands of **1**·4Cl and **2**·2Cl, exemplifying the lack of intermolecular dimer formation in **1**·4Cl or **2**·2Cl and providing evidence for the self-folding processes for these compounds.

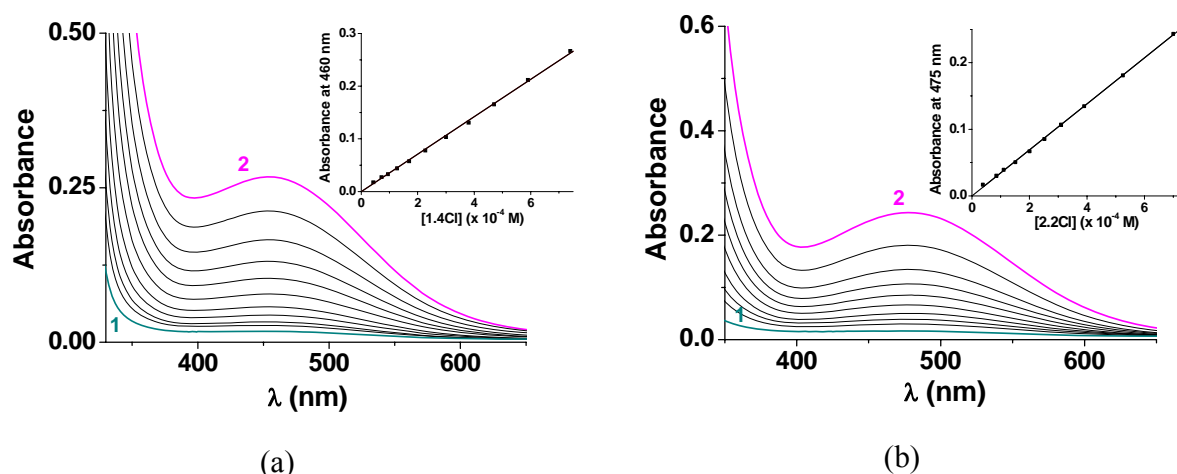


Figure S1. Absorption Spectrophotometric spectra of (a) **1**·4Cl and (b) **2**·2Cl showing the effect of dilution on the CT absorption bands. Solvent: H₂O, pH 7.0 (phosphate buffer 0.1 M), $T = 25.0(2) \text{ }^\circ\text{C}$. (a) 1: $[\mathbf{1}\cdot\mathbf{4Cl}] = 4.3 \times 10^{-5} \text{ M}$; 2: $[\mathbf{1}\cdot\mathbf{4Cl}] = 7.4 \times 10^{-4} \text{ M}$. (b) 1: $[\mathbf{2}\cdot\mathbf{2Cl}] = 3.8 \times 10^{-5} \text{ M}$; 2: $[\mathbf{2}\cdot\mathbf{2Cl}] = 7.0 \times 10^{-4} \text{ M}$. Insets show that the CT absorptions obey the Beer-Lambert law.

Figure S2 displays the spectral variation recorded on an equimolar mixture of **V·2Cl** and **N-1**. It clearly shows the absence of a CT complex between **V·2Cl** and **N-1** in the absence of **CB[8]**.

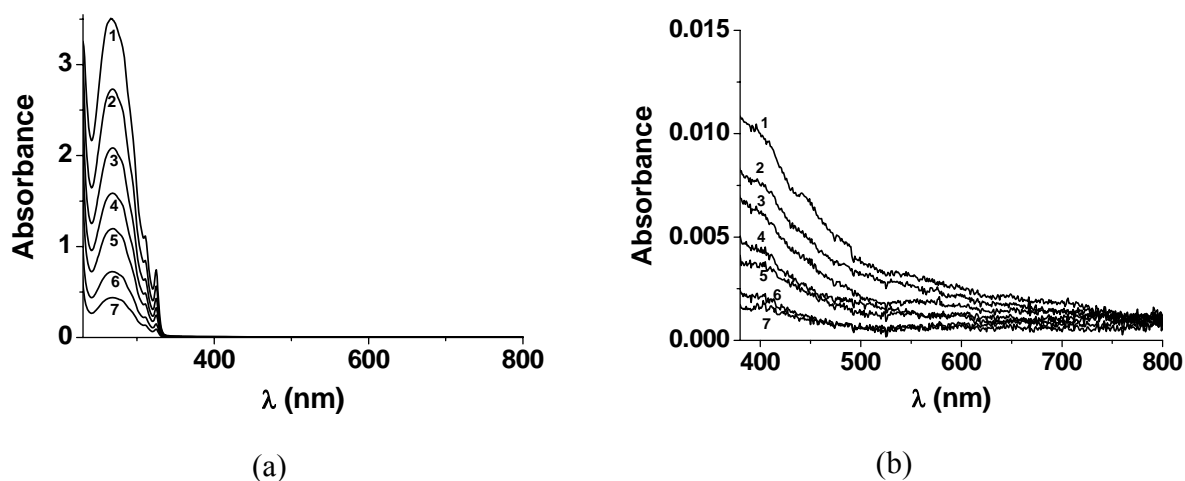


Figure S2. Absorption Spectrophotometric spectra of equimolar mixtures of **V·2Cl** and **N-1** at a variety of concentrations. Solvent: H_2O , pH 7.0 (phosphate buffer 0.1 M), $T = 25.0(2)^\circ\text{C}$, (1) 1.52×10^{-4} M, (2) 1.14×10^{-4} M, (3) 8.56×10^{-5} M, (4) 6.42×10^{-5} M, (5) 4.80×10^{-5} M, (6) 2.9×10^{-5} M, (7) 1.44×10^{-5} M. a) full spectral window, b) zoom-in of the visible region.

Spectroscopic Characterization of $\text{V}^{2+}\text{-CB[8]}$ Complex

The Job plot presented in **Figure S3** clearly confirms that a 1:1 complex is formed exclusively between **V·2Cl** and **CB[8]**.

Figure S3: Job plot ($\Delta A/\Delta A_{\text{max}}$ at 300 nm) obtained upon mixing **V·2Cl** and **CB[8]**. Solvent: H_2O ; $T = 25.0(0.2)^\circ\text{C}$; pH = 7.0 (phosphate buffer 0.1 M); $[\text{V}\cdot 2\text{Cl}]_{\text{tot}} + [\text{CB[8]}]_{\text{tot}} = 1.18 \times 10^{-4}$ M; $l = 0.5$ cm.

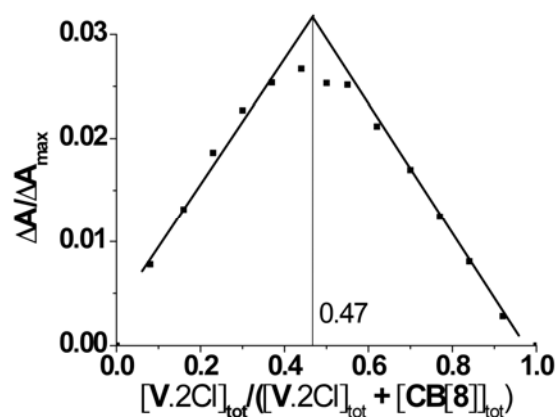


Figure S4 shows the electronic spectra of **V·2Cl**

and of its host-guest complex with **CB[8]**. The corresponding absorption spectrophotometric titration is given in Figure 2 in the manuscript. Inclusion of the dicationic viologen derivative within the macrocycle cavity results in a significant hypochromic shift of the main **V·2Cl** absorption band centered at 263 nm. A weak bathochromic shift of these π - π^* electronic transitions is also observed.

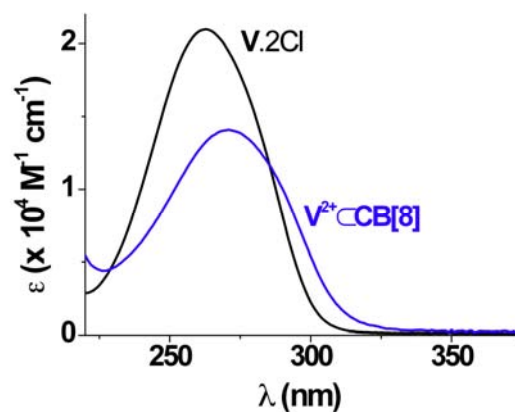
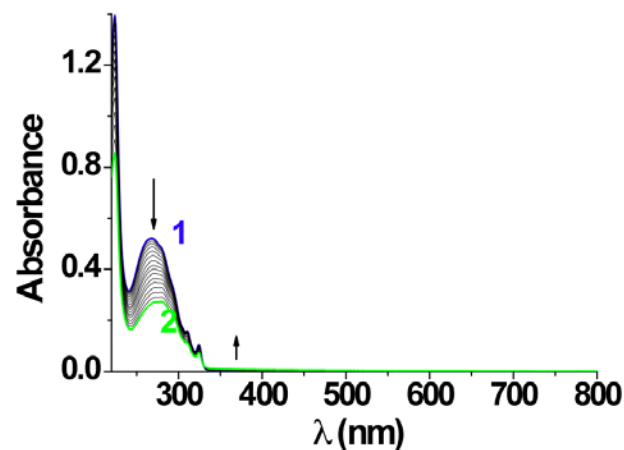


Figure S4: Absorption electronic spectra of **V·2Cl** and the **V²⁺⊂CB[8]** complex. Solvent: H₂O; pH = 7.00 (phosphate buffer 0.1 M); $T = 25.0(2)^\circ\text{C}$.

Absorption Spectrophotometric Titration of V·2Cl and N-1 by CB[8].

Figure S5 portrays the spectrophotometric titration of an equimolar mixture of **N-1** and **V·2Cl** by **CB[8]**.

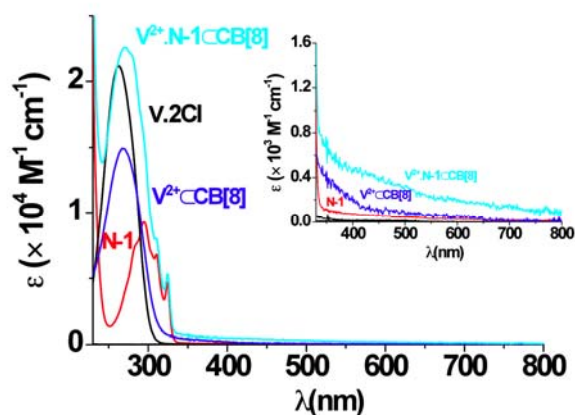
Figure S5: A UV-Visible absorption spectrophotometric titration of an equimolar mixture of **N-1** and **V·2Cl** with **CB[8]**. Solvent: H₂O; pH = 7.0 (phosphate buffer 0.1 M); $T = 25.0(2)^\circ\text{C}$; $[\text{V}\cdot 2\text{Cl}]_{\text{tot}} = 2.24 \times 10^{-5} \text{ M}$; $[\text{N-1}] = 2.26 \times 10^{-5} \text{ M}$ (1) $[\text{CB[8]}]_{\text{tot}} = 0$; (2) $[\text{CB[8]}]_{\text{tot}} = 9.53 \times 10^{-5} \text{ M}$; $l = 1 \text{ cm}$.



Spectroscopic Characterization of V²⁺·N-1⊂CB[8] Ternary Complex

Figure S6 presents the electronic spectra of **V·2Cl**, **N-1** and of the **V²⁺·N-1⊂CB[8]** ternary host-guest complex with **CB[8]**. The **V²⁺·N-1⊂CB[8]** ternary complex is characterized by the formation of a broad and weak CT absorption band at about 445 nm along with a significant hypochromic shift of the **V·2Cl**-centred absorption band with respect to the sum of **V·2Cl** and **N-1** electronic spectra. A weak bathochromic shift of the **V²⁺** π - π^* transitions with respect to those of **V·2Cl** and **V²⁺⊂CB[8]** is also observed.

Figure S6: Absorption electronic spectra of **V·2Cl** and **N-1** and of **V²⁺⊂CB[8]** and **V²⁺·N-1⊂CB[8]** complexes. Solvent: H₂O; pH = 7.0 (phosphate buffer 0.1 M); $T = 25.0(2)^\circ\text{C}$.

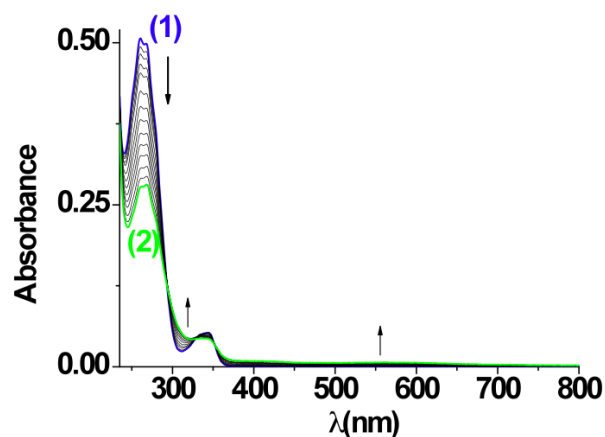


Absorption Spectrophotometric Titration

of V·2Cl and N-2 by CB[8]

Figure S7 illustrates the spectrophotometric titration of an equimolar mixture of N-2 and V·2Cl by CB[8].

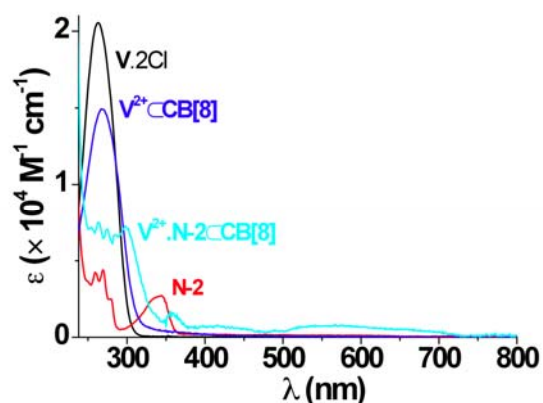
Figure S7: UV-Visible absorption spectrophotometric titration of an equimolar mixture of N-2 and V·2Cl with CB[8]. Solvent: H₂O; pH = 7.0 (phosphate buffer 0.1 M); T = 25.0(2)°C; [V·2Cl]_{tot} = 2.07 × 10⁻⁵ M; [N-2]_{tot} = 2.09 × 10⁻⁵ M; (1) [CB[8]]_{tot} = 0; (2) [CB[8]]_{tot} = 4.08 × 10⁻⁵ M; l = 1 cm.



Spectroscopic Characterization of V²⁺·N-1⊂CB[8] Ternary Complex

Figure S8 illustrates the electronic spectra of the V·2Cl and N-2 systems and of the V²⁺·N-2⊂CB[8] ternary host-guest complex. The ternary complex is characterized by the formation of a broad and a weak CT absorption band at about 570 nm along with significant hypochromic and bathochromic shifts of the V·2Cl-centred absorption band.

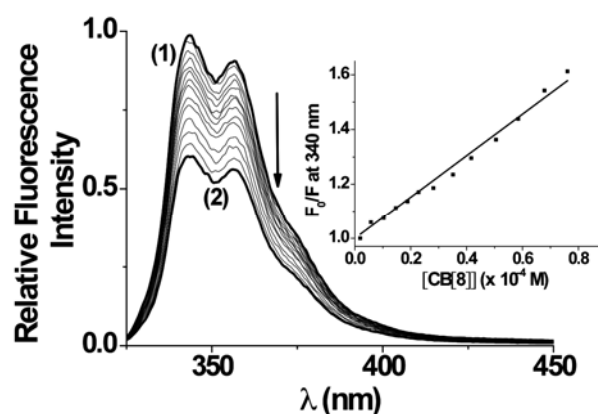
Figure S8: Absorption electronic spectra of V·2Cl and N-2 and of V²⁺⊂CB[8] and V²⁺·N-2⊂CB[8] complexes. Solvent: H₂O; pH = 7.0 (phosphate buffer 0.1 M) T = 25.0(2)°C.



Emission Spectrophotometric Titration of V·2Cl and N-1 by CB[8]

Figure S9 describes the spectrofluorimetric titration of an equimolar mixture of N-1 and V·2Cl by CB[8]. These excited state data have been analyzed according to Stern-Volmer approach (see figure in the inset).

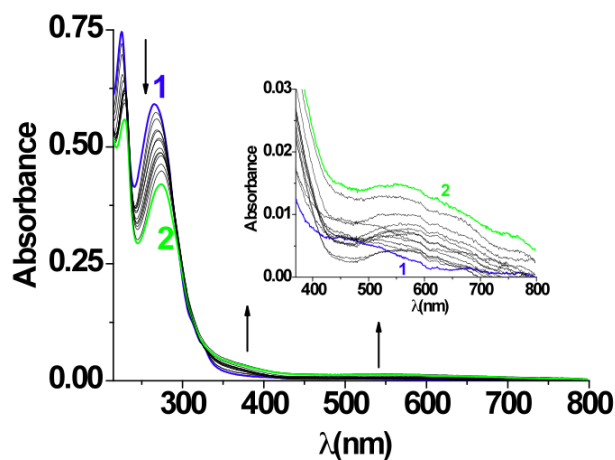
Figure S9: Spectrofluorimetric titration of an equimolar mixture of N-1 and V·2Cl with CB[8]. Solvent: water; pH = 7.00 (phosphate buffer 0.1 M); $T = 25.0(2)^{\circ}\text{C}$; $[\text{V}\cdot 2\text{Cl}]_{\text{tot}} = [\text{N}\cdot 1] = 1.51 \times 10^{-5} \text{ M}$; (1) $[\text{CB}[8]]_{\text{tot}} = 0$; (2) $[\text{CB}[8]]_{\text{tot}} = 7.6 \times 10^{-5} \text{ M}$; $\lambda_{\text{exc}} = 325 \text{ nm}$; $l = 1 \text{ cm}$; emission and excitation slit widths = 5 nm. Inset: Stern-Volmer analysis ($F_0/F = 1 + K_{\text{V}^{2+}, \text{N}\cdot 1} \text{CB}[8] \times [\text{CB}[8]]$) at $\lambda = 340 \text{ nm}$.



Absorption Spectrophotometric Titration of 1·4Cl by CB[8]

Figure S10 describes the spectrophotometric titration of the thread 1·4Cl with CB[8]. Statistical processing of these data allowed us to calculate the electronic spectra of $1^{4+} \subset \text{CB}[8]$ and $1^{4+} \subset (\text{CB}[8])_2$. They are available in Figure 7b.

Figure S10: UV-Visible absorption spectrophotometric titration of 1·4Cl with CB[8]. Solvent: H₂O; pH = 7.0 (phosphate buffer 0.1 M); $T = 25.0(2)^{\circ}\text{C}$; $[1\cdot 4\text{Cl}]_{\text{tot}} = 9.36 \times 10^{-6} \text{ M}$; (1) $[\text{CB}[8]]_{\text{tot}} / [1\cdot 4\text{Cl}]_{\text{tot}} = 0$; (2) $[\text{CB}[8]]_{\text{tot}} / [1\cdot 4\text{Cl}]_{\text{tot}} = 18.6$; $l = 1 \text{ cm}$.



Absorption Spectrophotometric Titration

of 2·2Cl by CB[8]

Figure S11 describes the spectrophotometric titration of thread 2·2Cl by CB[8]. Statistical processing of these data allowed us to calculate the electronic spectrum of $2^{2+} \subset \text{CB}[8]$, which is available in Figure 7a.

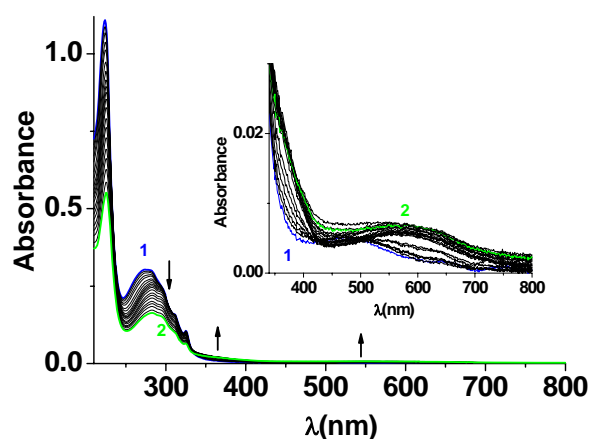
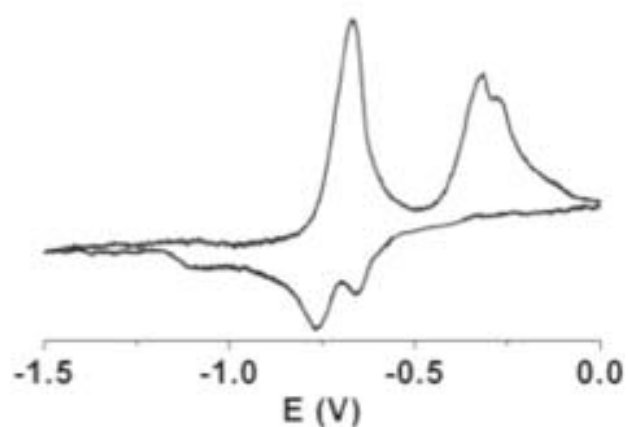


Figure S11: UV-Vis absorption spectrophotometric titration of 2·2Cl with CB[8]. Solvent: H₂O; pH = 7.0 (phosphate buffer 0.1 M); $T = 25.0(2)^\circ\text{C}$; $[2\cdot 2\text{Cl}]_{\text{tot}} = 1.32 \times 10^{-5} \text{ M}$; (1) $[\text{CB}[8]]_{\text{tot}} / [2\cdot 2\text{Cl}]_{\text{tot}} = 0$; (2) $[\text{CB}[8]]_{\text{tot}} / [2\cdot 2\text{Cl}]_{\text{tot}} = 6.7$; $l = 1 \text{ cm}$.

Switching Properties of the [2]Pseudorotaxanes

A cyclic voltammogram of $2^{2+} \subset \text{CB}[8]$ recorded at $50 \text{ mV}\cdot\text{s}^{-1}$ shows further evidence of a peak at -1.20 V characteristic of the dimerization of viologen units in the cavity of CB[8].

Figure S12: Cyclic voltammograms of 3·2Cl (1mM) with a scan rate = $50 \text{ mV}\cdot\text{s}^{-1}$ in H₂O, pH = 7.0 (phosphate buffer 0.1 M).



NMR Spectroscopic Investigations

Complexes $1^{4+} \subset \text{CB}[8]$ and $2^{2+} \subset \text{CB}[8]$ were also examined by ^1H NMR spectroscopy (Figures S13 and S14). Assignments of the peaks in the NMR spectrum for their respective compounds, $1 \cdot 4\text{Cl}$ and $2 \cdot 2\text{Cl}$, were aided by 2D NMR techniques. The 1D ^1H NMR spectra supports the formation of 1:1 complexation for $1 \cdot 4\text{Cl}$ and $2 \cdot 2\text{Cl}$ with $\text{CB}[8]$. Examining the resonances for compound $1 \cdot 4\text{Cl}$ confirms the C_2 symmetry around the central naphthalene unit. Upon addition of $\text{CB}[8]$ the C_2 axis is nullified and provides for structurally different viologen units as well as a doubling of the naphthalene resonances in the formation of $1^{4+} \subset \text{CB}[8]$. Additionally, the naphthalene resonances are all shifted upfield ~ 0.6 ppm, consistent with naphthalene as a guest for $\text{CB}[8]$. Splitting of the four viologen units indicates, not only two structurally different viologens, but also an additional loss of symmetry for the encircled viologens (**Figure S13**). Upon addition of extra equivalents of $\text{CB}[8]$, significant broadening of the viologen signals is observed; a phenomenon which supports the UV/Vis spectroscopic data, indicating an additional binding site (albeit much weaker) for $\text{CB}[8]$. Similar information is gleaned from the NMR spectrum of $2^{2+} \subset \text{CB}[8]$ (**Figure S14**). Again, the C_2 axis of the thread ($2 \cdot 2\text{Cl}$) is destroyed upon addition of $\text{CB}[8]$. In response to this loss of symmetry, the single (formerly symmetric) viologen unit is split into four broad singlets and the naphthalene units split into encircled and unencircled resonances. Encircled naphthalene manifests an upfield shift of ~ 0.7 - 1.5 ppm.

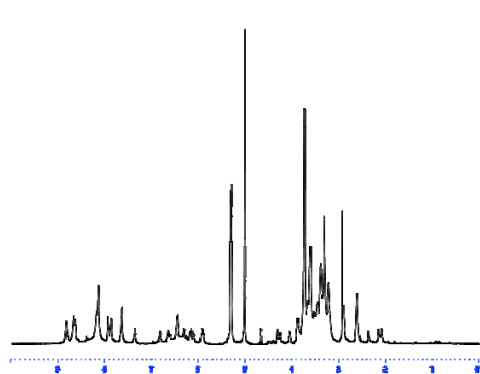


Figure S13: ^1H NMR Spectrum of $1^{4+} \subset \text{CB}[8]$ in D_2O at 275K

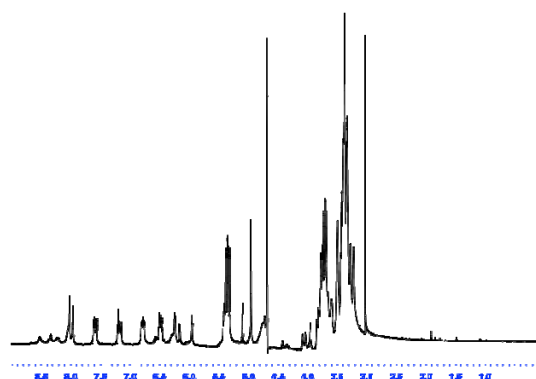


Figure S14: ^1H NMR Spectrum of $2^{2+} \subset \text{CB}[8]$ in D_2O at 280K